

# A Deep Learning Algorithm for High-Dimensional Exploratory Item Factor Analysis

Christopher J. Urban\* and Daniel J. Bauer

*L.L. Thurstone Psychometric Laboratory in the  
Department of Psychology and Neuroscience  
University of North Carolina at Chapel Hill  
Chapel Hill, NC 27599*

March 27, 2022

## Abstract

Deep learning methods are the gold standard for non-linear statistical modeling in computer vision and in natural language processing but are rarely used in psychometrics. To bridge this gap, we present a novel deep learning algorithm for exploratory item factor analysis (IFA). Our approach combines a deep artificial neural network (ANN) model called a variational autoencoder (VAE) with recent work that uses regularization for exploratory factor analysis. We first provide overviews of ANNs and VAEs. We then describe how to conduct exploratory IFA with a VAE and demonstrate our approach in two empirical examples and in two simulated examples. Our empirical results were consistent with existing psychological theory across random starting values. Our simulations suggest that the VAE consistently recovers the data generating factor pattern with moderate-sized samples. Secondary loadings were underestimated with a complex factor structure and intercept parameter estimates were moderately biased with both simple and complex factor structures. All models converged in minutes, even with hundreds of thousands of observations, hundreds of items, and tens of factors. We conclude that the VAE offers a powerful new approach to fitting complex statistical models in psychological and educational measurement.

**Keywords:** Deep learning, artificial neural networks, variational autoencoders, regularization, item response theory, categorical factor analysis, latent variable modeling

---

\*Correspondence to [cjurban@live.unc.edu](mailto:cjurban@live.unc.edu).

# 1 Introduction

*Item factor analysis* (IFA) is a popular method for summarizing a number of categorical item responses using a smaller number of continuous latent variables. It is an indispensable tool for item analysis as well as test construction and scoring in psychological and educational measurement research (Bolt, 2005; Wirth & Edwards, 2007). Although traditional IFA models only included one latent variable (e.g., Lord, Novick, & Birnbaum, 1968), applications of IFA to topics like health outcomes and personality psychology combined with advances in computing spurred the development of multidimensional IFA models with many latent variables (e.g., Bjorner, Chang, Thissen, & Reeve, 2007; Reeve et al., 2007). In theory, maximum likelihood estimation (MLE) for multidimensional IFA model parameters is possible using Bock and Aitkin’s (1981) maximum marginal likelihood (MML) estimator. In practice, however, the MML approach writes IFA model likelihoods as analytically intractable integrals that are computationally burdensome to evaluate in the high-dimensional setting (i.e., when the number of latent variables is large). Cai (2010a, 2010b) reviews research efforts to avoid this computational burden, which is called the *curse of dimensionality*.

The *Metropolis-Hastings Robbins-Monro* (MH-RM) algorithm (Cai, 2010a, 2010b) was a breakthrough in the struggle with the curse of dimensionality and is currently the most efficient algorithm for MLE in high-dimensional IFA. Briefly, MH-RM iteratively imputes unobserved latent variable values with a Metropolis-Hastings sampler (Hastings, 1970; Metropolis, Rosenbluth, Rosenbluth, Teller, & Teller, 1953) then updates IFA model parameters with the Robbins-Monro algorithm (Robbins & Monro, 1951). MH-RM is orders of magnitude faster than other estimation approaches when the latent space is high-dimensional.

Despite advances such as MH-RM, MLE procedures for high-dimensional IFA that scale to very large samples have not been developed. In this paper, we develop such a procedure using *deep learning* (DL), a machine learning approach that extracts information from data using many layers of processing (Goodfellow, Bengio, & Courville, 2016; Urban & Gates, 2019). Our procedure is based on the *variational autoencoder* (VAE), a deep *artificial neural network* (ANN) model originally developed for generating realistic images (Kingma & Welling, 2013; Rezende, Mohamed, & Wierstra, 2014). In addition to scaling to large samples, our approach offers ancillary benefits including (1) iterative parameter estimate updates as new data is collected, (2) non-linear factor score estimation using ANNs, (3) convergence to high-quality optima using recent stochastic optimization techniques, and (4) support by an active DL literature that may offer improvements leading to better modeling and estimation in many contexts.

Our work extends that of Curi, Converse, and Hajewski (2019), who used a VAE to estimate item parameters in a confirmatory multidimensional two-parameter logistic (M2PL) model. Curi et al. suggest that with moderate-sized samples (e.g.,  $N = 500$  to  $N = 5,000$ ), the VAE is less accurate but converges much faster than traditional estimation methods like Markov chain Monte Carlo (MCMC; Gelfand & Smith, 1990). Specifically, their model achieved an approximately  $40\times$  speedup with a sample size  $20\times$  larger than MCMC. We

anticipate that the VAE can be optimized to improve accuracy with moderate-sized samples.

The goal of our paper is to demonstrate the advantages of VAEs for IFA. We focus on exploratory applications in which the number of factors and the structure of the factor pattern matrix are not specified *ex ante*. Section 2 introduces the problem of fitting IFA models with graded responses. Section 3 provides a brief overview of ANNs. Section 4 discusses VAEs. Section 5 shows how VAEs can be modified in ways designed to allow for ordered categorical item responses, permit correlated factors, and improve accuracy. Section 6 demonstrates our VAE approach in two empirical examples and in two simulation studies.

## 2 The Problem of Fitting High-Dimensional Item Factor Analysis Models

### 2.1 The Graded Item Response Model

This section introduces notation for Samejima’s (1969) graded response model (GRM) following Cai (2010b). Let  $i = 1, \dots, N$  index independent respondents and  $j = 1, \dots, n$  index items. Let item  $j$  have  $C_j$  graded response categories. Let  $y_{i,j}$  denote respondent  $i$ ’s response to item  $j$ . Suppose we have  $p$  latent variables; let  $\mathbf{x}_i$  denote the  $p \times 1$  vector of factor scores (i.e., latent variable values) for respondent  $i$ . Let  $\boldsymbol{\beta}_j$  denote the  $p \times 1$  vector of loadings, let  $\boldsymbol{\alpha}_j = (\alpha_{j1}, \dots, \alpha_{j,C_j-1})^\top$  denote the  $(C_j - 1) \times 1$  vector of strictly ordered category intercepts, and let  $\boldsymbol{\theta}_j = (\boldsymbol{\alpha}_j^\top, \boldsymbol{\beta}_j^\top)^\top$  be a vector collecting all parameters for item  $j$ . Define a set of boundary response probabilities conditional on the item parameters  $\boldsymbol{\theta}_j$  and the factor scores  $\mathbf{x}_i$ :

$$P(y_{i,j} \geq k \mid \boldsymbol{\theta}_j, \mathbf{x}_i) = P_{i,j,k} = \frac{1}{1 + \exp(-D(\alpha_{j,k} + \boldsymbol{\beta}_j^\top \mathbf{x}_i))}, \quad (1)$$

where  $k \in \{0, \dots, C_j - 1\}$  and  $D = 1$  is a scaling constant. The conditional probability for a particular response  $y_{i,j} = k$  is

$$\pi_{i,j,k} = P(y_{i,j} = k \mid \boldsymbol{\theta}_j, \mathbf{x}_i) = P_{i,j,k} - P_{i,j,k+1}, \quad (2)$$

where  $P_{i,j,0} = 1$  and  $P_{i,j,C_j} = 0$ .

### 2.2 Observed Data Likelihood

To fit the GRM, we must obtain the likelihood of the observed data. From equation 2, the conditional distribution of each  $y_{i,j}$  is multinomial with  $C_j$  cells, cell probabilities  $\pi_{i,j,k}$ , and trial size 1:

$$p(y_{i,j} \mid \boldsymbol{\theta}_j, \mathbf{x}_i) = \prod_{k=0}^{C_j-1} \pi_{i,j,k}^{\mathbf{1}_k(y_{i,j})}, \quad (3)$$

where the term in the exponent is the indicator function

$$\mathbb{1}_k(y) = \begin{cases} 1, & \text{if } y = k \\ 0, & \text{otherwise} \end{cases} \quad (4)$$

for  $k \in \{0, 1, \dots\}$ . Let  $\mathbf{y}_i = (y_{i,1}, \dots, y_{i,n})^\top$  be respondent  $i$ 's response pattern. Invoking the usual conditional independence assumption,  $\mathbf{y}_i$  has conditional density

$$p(\mathbf{y}_i | \boldsymbol{\theta}, \mathbf{x}_i) = \prod_{j=1}^n p(y_{i,j} | \boldsymbol{\theta}_j, \mathbf{x}_i), \quad (5)$$

where  $\boldsymbol{\theta}$  is a  $d \times 1$  vector collecting the item parameters for all  $n$  items.

Assume the factor scores  $\mathbf{x}_i$  follow a multivariate normal distribution with mean vector  $\boldsymbol{\mu}$  and covariance matrix  $\boldsymbol{\Sigma}$ . We write the cumulative distribution function of  $\mathbf{x}_i$  as  $\Phi(\mathbf{x}_i | \boldsymbol{\mu}, \boldsymbol{\Sigma})$  and the density function as  $\phi(\mathbf{x}_i | \boldsymbol{\mu}, \boldsymbol{\Sigma})$ . The marginal density of  $\mathbf{y}_i$  is

$$p(\mathbf{y}_i | \boldsymbol{\theta}) = \int \prod_{j=1}^n p(y_{i,j} | \boldsymbol{\theta}_j, \mathbf{x}_i) \Phi(\mathbf{x}_i | \boldsymbol{\mu}, \boldsymbol{\Sigma}) d\mathbf{x}_i. \quad (6)$$

Finally, letting  $\mathbf{Y}$  be an  $N \times n$  matrix of independent response patterns whose  $i^{\text{th}}$  row is  $\mathbf{y}_i^\top$ , the observed data likelihood is

$$\mathcal{L}(\boldsymbol{\theta} | \mathbf{Y}) = \prod_{i=1}^N \left[ \int \prod_{j=1}^n p(y_{i,j} | \boldsymbol{\theta}_j, \mathbf{x}_i) \Phi(\mathbf{x}_i | \boldsymbol{\mu}, \boldsymbol{\Sigma}) d\mathbf{x}_i \right]. \quad (7)$$

Maximizing  $\mathcal{L}(\boldsymbol{\theta} | \mathbf{Y})$  in equation 7 directly gives the MML estimator  $\hat{\boldsymbol{\theta}}$ . However, this maximization is difficult because  $\mathcal{L}(\boldsymbol{\theta} | \mathbf{Y})$  cannot be simplified further analytically. Instead, we need to approximate the  $N$  integrals over  $\mathbb{R}^p$  in equation 7 numerically. In this paper, we avoid this problem by writing an analytical lower bound on  $\mathcal{L}(\boldsymbol{\theta} | \mathbf{Y})$  using a technique called *variational inference*. We then optimize this lower bound using a DL approach.

### 3 A Brief Overview of Artificial Neural Networks

*Deep learning* (DL) is a machine learning approach that maps a set of predictors through a sequence of transformations called *layers* to predict a set of outcomes. *Artificial neural networks* (ANNs) are a class of non-linear statistical models that have been remarkably successful under the DL framework. When composed together in many layers, ANNs are feasible to fit and often obtain high predictive accuracy (Goodfellow et al., 2016; Urban & Gates, 2019). This section briefly discusses ANNs, which are the building blocks of VAEs, as well as ANN fitting methods.

### 3.1 Feedforward Neural Networks

*Feedforward neural networks* (FNNs) are the simplest ANNs. In practice, FNNs are used as flexible, scalable function approximators because they can approximate any Borel-measurable function between finite-dimensional spaces to any non-zero amount of error (e.g., Lu, Pu, Wang, Hu, & Wang, 2017).

Consider a data set  $\{\mathbf{y}_i, \mathbf{x}_i\}_{i=1}^N$  where  $\mathbf{y}_i$  is the  $i^{\text{th}}$  observed  $n \times 1$  vector of dependent variables and  $\mathbf{x}_i$  is the  $i^{\text{th}}$  observed  $p \times 1$  vector of independent variables. Note that here  $\mathbf{x}_i$  denotes set of observed variables in line with typical DL applications, although we will later re-define  $\mathbf{x}_i$  as a set of latent variables. The FNN maps the predictors  $\mathbf{x}_i$  through a sequence of  $L$  non-linear transformations to predict the outcomes  $\mathbf{y}_i$ . These transformations are given by

$$\mathbf{h}_i^{(l)} = \psi^{(l)}(\mathbf{W}^{(l)}\mathbf{h}_i^{(l-1)} + \mathbf{b}^{(l)}), \quad l = 1, \dots, L, \quad (8)$$

where  $\mathbf{h}_i^{(1)} = \mathbf{x}_i$ ,  $\mathbf{h}_i^{(L)} = \mathbf{y}_i - \boldsymbol{\varepsilon}_i$  where  $\boldsymbol{\varepsilon}_i$  is the  $i^{\text{th}}$  observed  $n \times 1$  vector of error variables,  $\mathbf{h}_i^{(l)}$  is a  $p_l \times 1$  vector of *derived predictor* values for layers  $l = 2, \dots, L - 1$ ,  $\mathbf{W}^{(l)}$  is a  $p_l \times p_{l-1}$  regression weight matrix for layer  $l$ ,  $\mathbf{b}^{(l)}$  is a  $p_l \times 1$  intercept vector for layer  $l$ , and  $\psi^{(l)}(\cdot)$  is a non-linear *activation function* for layer  $l$ . Equation 8 is essentially a recursive generalized linear model where  $\psi^{(l)}(\cdot)$  corresponds to an inverse link function linking a linear combination of the layer  $l - 1$  derived predictors to the mean of the layer  $l$  derived predictors. Figure 1 shows a schematic diagram of an FNN with  $i$  subscripts omitted to avoid clutter. Notice that  $\mathbf{x}$  and  $\mathbf{y}$  are called the *input layer* and the *output layer*, respectively, while intermediate layers are called *hidden layers*.

The hidden layer activation functions  $\psi^{(1)}(\cdot), \psi^{(2)}(\cdot), \dots, \psi^{(L-1)}(\cdot)$  are typically the *rectified linear unit* (ReLU) function

$$\psi(z) = \max(0, z), \quad (9)$$

which is applied to vectors element-wise. ANNs with ReLU hidden layers are easy to fit and often perform well (e.g., Glorot, Bordes, & Bengio, 2011; Jarrett, Kavukcuoglu, Ranzato, & LeCun, 2009; Nair & Hinton, 2010). Our choice for the final activation function  $\psi^{(L)}(\cdot)$  depends on the outcomes. For example, if the outcomes are dichotomous, we choose  $\psi^{(L)}(\cdot)$  to be the inverse logit function

$$\psi(z) = \frac{1}{1 + \exp(-z)}, \quad (10)$$

which is applied to vectors element-wise and corresponds to a logistic regression of the outcomes on the layer  $L - 1$  derived predictors. We consider the case of polytomous outcomes when we discuss using VAEs to fit the GRM in Section 5.

### 3.2 Fitting FNNs Using Stochastic Gradient Descent

Fitting FNNs starts with an objective function that measures model performance. We write this objective function as  $J(\boldsymbol{\gamma})$  where  $\boldsymbol{\gamma}$  is an  $r \times 1$  vector containing

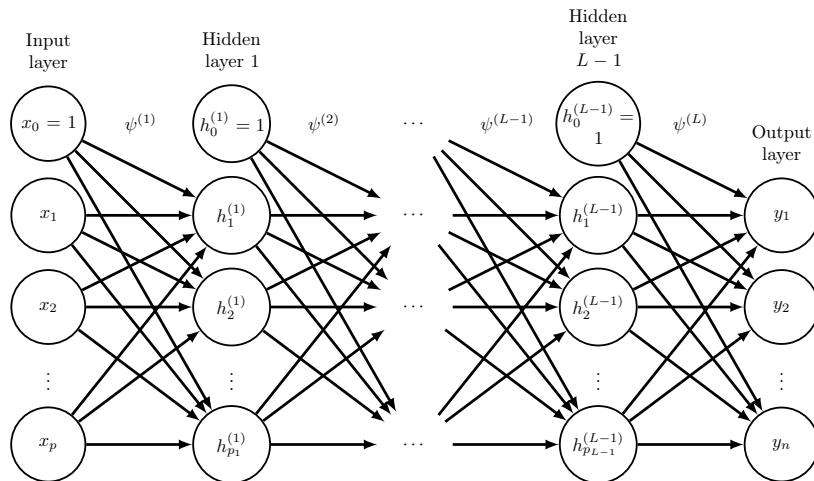


**Figure 1:** Schematic representation of a feedforward neural network with  $L$  layers. Edges represent functions and nodes represent elements of vector-valued layers. Intercepts are included by multiplying the intercepts by new nodes  $x_0, h_0^{(1)}, \dots, h_0^{(L-1)}$  that are equal to one.

the FNN parameters. Model fitting consists of solving the equations produced by setting the gradient of  $J(\gamma)$  to zero:

$$\nabla_{\gamma} J(\gamma) = 0, \quad (11)$$

where  $\nabla_{\gamma}$  returns an  $r \times 1$  vector of first-order partial derivatives of  $J(\gamma)$  w.r.t.  $\gamma$ . In practice, finding a closed-form solution for the global minimum of equation 11 is challenging because  $J(\gamma)$  is often non-convex with many local stationary points. We may instead use *gradient descent* (GD) to find a local minimum with  $J(\gamma)$  reasonably small. GD proposes recursive parameter updates as

$$\gamma_{k+1} = \gamma_k - \eta \nabla_{\gamma} J(\gamma_k), \quad (12)$$

where  $\eta \in \mathbb{R}_+$  is called the *learning rate*. With certain assumptions on  $J(\gamma)$  and on  $\eta$ , convergence to a local minimum is guaranteed for non-convex  $J(\gamma)$  (e.g., Lee, Simchowitz, Jordan, & Recht, 2016).

GD becomes computationally burdensome with large data sets. To see this, assume that the objective function decomposes as a sum over observations:

$$J(\gamma) = \frac{1}{N} \sum_{i=1}^N J_i(\gamma), \quad (13)$$

where  $J_i(\gamma)$  is a per-observation objective function. Each GD iteration computes

$$\nabla_{\gamma} J(\gamma) = \frac{1}{N} \sum_{i=1}^N \nabla_{\gamma} J_i(\gamma), \quad (14)$$

which is prohibitively slow for large  $N$ .

*Stochastic gradient descent* (SGD) alleviates this computational burden by noting that, for additive objective functions, the gradient of the per-observation objective  $J_i(\boldsymbol{\gamma})$  for a single observation is an unbiased estimator for the gradient of the full data set objective  $J(\boldsymbol{\gamma})$ :

$$\mathbb{E}(\nabla_{\boldsymbol{\gamma}} J_i(\boldsymbol{\gamma})) = \nabla_{\boldsymbol{\gamma}} J(\boldsymbol{\gamma}), \quad (15)$$

with the expectation taken w.r.t. the empirical density. SGD passes through the full data set, sampling single observations and updating parameters recursively:

$$\boldsymbol{\gamma}_{k+1} = \boldsymbol{\gamma}_k - \eta_k \nabla_{\boldsymbol{\gamma}} J_i(\boldsymbol{\gamma}), \quad (16)$$

where the learning rate now depends on the iteration  $k$ . The gradient computation at each step in equation 16 is clearly less burdensome at each iteration than the computation in equation 14. For large  $N$ , SGD may converge more quickly than GD and may even converge before encountering every observation in the data set. See Bottou and Bousquet (2011) for an asymptotic analysis of the relative convergence rates of GD and SGD.

The SGD estimator has high variance. To reduce this variance, we can average the per-observation objective gradients for a subsample of observations called a *mini-batch*. For a mini-batch  $\{\mathbf{y}_i, \mathbf{x}_i\}_{i=1}^m$  with  $m < N$ , an estimator of the gradient of the full data set objective is

$$\mathbf{g} = \frac{1}{m} \nabla_{\boldsymbol{\gamma}} \sum_{i=1}^m J_i(\boldsymbol{\gamma}). \quad (17)$$

Typically, mini-batches are sampled uniformly at random without replacement. After one pass through the full data set, called an *epoch*, we randomly shuffle the data and make further passes. Mini-batch SGD updates parameters recursively:

$$\boldsymbol{\gamma}_{k+1} = \boldsymbol{\gamma}_k - \eta_k \mathbf{g}. \quad (18)$$

Mini-batch SGD corresponds to a tradeoff between the low variance of GD and the computational efficiency of SGD. The mini-batch approach is used in most DL applications (Bottou, Curtis, & Nocedal, 2018). However, convergence to a local minimum is challenging to prove for mini-batch SGD as used in practice (although see Shamir (2016) and Jain, Nagaraj, and Netrapalli (2019)).

For FNNs, computing the gradient  $\mathbf{g}$  in equation 16 relies on an algorithm called *backpropagation* (BP). BP is an efficient application of the chain rule of calculus that is known as *reverse mode differentiation* in other fields (Griewank, 2012). See Goodfellow et al. (2016) for an in-depth discussion of BP.

## 4 Variational Autoencoders

In this section, we first describe an ANN-based latent variable model called an autoencoder (AE). We then explain variational inference (VI), a technique for approximate MLE in general latent variable models. Finally, we present VAEs, which are AEs that perform VI.

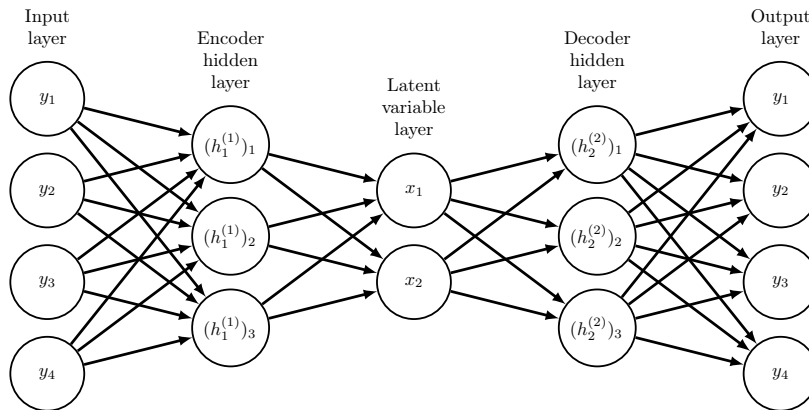


**Figure 2:** Schematic representation of an autoencoder with a single-layer encoder and a single-layer decoder. Intercepts are omitted to avoid clutter.

## 4.1 Autoencoders

*Autoencoders* (AEs) are ANNs that copy their input to their output. Internally, AEs first map their input to a vector of latent variables, then reconstruct their input from the latent vector. We will see that VAEs are essentially AEs with strong assumptions on the latent distribution.

AEs consist of two FNNs: An *encoder* FNN maps the input to the latent vector, and a *decoder* FNN maps the latent vector to the reconstructed input. Consider a data set  $\{\mathbf{y}_i\}_{i=1}^N$  where  $\mathbf{y}_i$  is the  $i^{\text{th}}$   $n \times 1$  vector of observed variables. The AE model is given by

$$\begin{aligned} \mathbf{x}_i &= \text{EncoderFNN}(\mathbf{y}_i; \boldsymbol{\gamma}_1) \\ \hat{\mathbf{y}}_i &= \text{DecoderFNN}(\mathbf{x}_i; \boldsymbol{\gamma}_2) + \boldsymbol{\varepsilon}_i, \end{aligned} \quad (19)$$

where  $\mathbf{x}_i$  is an unobserved  $p \times 1$  vector of latent variables with  $p < n$ ,  $\boldsymbol{\gamma}_1$  is an  $r_1 \times 1$  parameter vector,  $\boldsymbol{\gamma}_2$  is an  $r_2 \times 1$  parameter vector,  $\text{EncoderFNN}(\cdot; \boldsymbol{\gamma}_1)$  is an FNN with  $L_1$  layers parameterized by  $\boldsymbol{\gamma}_1$ ,  $\text{DecoderFNN}(\cdot; \boldsymbol{\gamma}_2)$  is an FNN with  $L_2$  layers parameterized by  $\boldsymbol{\gamma}_2$ , and  $\boldsymbol{\varepsilon}_i$  is the  $i^{\text{th}}$  observed  $n \times 1$  vector of error variables. No distributional assumptions are made on the latent variables  $\mathbf{x}_i$ .

The AE objective function penalizes the  $n \times 1$  reconstructed input vector  $\hat{\mathbf{y}}_i$  for being dissimilar to  $\mathbf{y}_i$ . For example, we typically use the mean squared error (MSE) objective with continuous  $\mathbf{y}_i$ :

$$\text{MSE}(\boldsymbol{\gamma}_1, \boldsymbol{\gamma}_2) = \frac{1}{N} \sum_{i=1}^N \|\mathbf{y}_i - \hat{\mathbf{y}}_i\|_2^2. \quad (20)$$

The objective can be optimized using mini-batch SGD and BP. Figure 2 visualizes an AE whose encoder and decoder both have one hidden layer.



## 4.2 Variational Inference

*Variational inference* (VI) is an approach to approximate MLE for latent variable models (Blei, Kucukelbir, & McAuliffe, 2017; Zhang, Butepage, Kjellstrom, & Mandt, 2019). We now use VI to derive an analytic lower bound on the observed data likelihood. This lower bound will serve as the VAE objective function.

Let  $\mathbf{Y}$  denote the  $N \times n$  matrix of observations whose  $i^{\text{th}}$  row is the  $1 \times n$  observed vector  $y_i^\top$  and let  $\mathbf{X}$  denote the  $N \times p$  matrix of latent variables whose  $i^{\text{th}}$  row is the  $1 \times p$  factor score vector  $\mathbf{x}_i^\top$ . We want the latent variable posterior  $p(\mathbf{X} | \mathbf{Y})$  so we can do inference over  $\mathbf{X}$ .  $p(\mathbf{X} | \mathbf{Y})$  is given by

$$p(\mathbf{X} | \mathbf{Y}) = \frac{p(\mathbf{X}, \mathbf{Y})}{p(\mathbf{Y})}. \quad (21)$$

The observed data likelihood  $p(\mathbf{Y})$  is called the *evidence* in VI and is given by<sup>1</sup>

$$p(\mathbf{Y}) = \int p(\mathbf{X}, \mathbf{Y}) d\mathbf{X}. \quad (22)$$

This integral is analytically intractable for many models (e.g., the GRM), making it hard to compute the posterior and to do inference over the latent variables.

VI approaches this problem by approximating the true posterior  $p(\mathbf{X} | \mathbf{Y})$ . Specifically, VI proposes a family of densities  $Q$  such that each  $q(\mathbf{X} | \mathbf{Y}) \in Q$  is a candidate approximation to  $p(\mathbf{X} | \mathbf{Y})$ . If we measure the difference between  $q(\mathbf{X} | \mathbf{Y})$  and  $p(\mathbf{X} | \mathbf{Y})$  using the *Kullback-Leibler* (KL) *divergence*<sup>2</sup>, our problem amounts to solving the optimization problem

$$q^*(\mathbf{X} | \mathbf{Y}) = \arg \min_{q(\mathbf{X} | \mathbf{Y}) \in Q} D_{\text{KL}}(q(\mathbf{X} | \mathbf{Y}) || p(\mathbf{X} | \mathbf{Y})), \quad (23)$$

where the KL divergence is

$$D_{\text{KL}}(q(\mathbf{X} | \mathbf{Y}) || p(\mathbf{X} | \mathbf{Y})) = \mathbb{E}(\log q(\mathbf{X} | \mathbf{Y})) - \mathbb{E}(\log p(\mathbf{X} | \mathbf{Y})) \quad (24)$$

with expectations taken w.r.t.  $q(\mathbf{X} | \mathbf{Y})$ .

We cannot directly compute the KL divergence in equation 24 because it depends on the intractable  $p(\mathbf{Y})$ . This can be seen by expanding the posterior:

$$D_{\text{KL}}(q(\mathbf{X} | \mathbf{Y}) || p(\mathbf{X} | \mathbf{Y})) = \mathbb{E}(\log q(\mathbf{X} | \mathbf{Y})) - \mathbb{E}(\log p(\mathbf{X}, \mathbf{Y})) + \log p(\mathbf{Y}). \quad (25)$$

Since  $p(\mathbf{Y})$  does not depend on  $\mathbf{X}$ , we can optimize an alternative objective called the *evidence lower bound* (ELBO):

$$\text{ELBO}(q) = \mathbb{E}(\log p(\mathbf{X}, \mathbf{Y})) - \mathbb{E}(\log q(\mathbf{X} | \mathbf{Y})). \quad (26)$$

Maximizing the ELBO is equivalent to the minimization in equation 23.

<sup>1</sup>We use  $\int \cdot d\mathbf{X}$  as shorthand for  $\int \dots \int \cdot dx_1 \dots dx_N$ .

<sup>2</sup>The KL divergence  $D_{\text{KL}}(q||p)$  measures how different distribution  $q$  is from reference distribution  $p$ . It is nonnegative (i.e.,  $D_{\text{KL}}(q||p) \geq 0$ ), asymmetric (i.e.,  $D_{\text{KL}}(q||p) \neq D_{\text{KL}}(p||q)$ ), and is minimized when  $q(\cdot) = p(\cdot)$ .

To better understand how  $q^*(\mathbf{X} | \mathbf{Y})$  is chosen, we can re-write the ELBO:

$$\text{ELBO}(q) = \mathbb{E}(\log p(\mathbf{X})) + \mathbb{E}(\log p(\mathbf{Y} | \mathbf{X})) - \mathbb{E}(\log q(\mathbf{X} | \mathbf{Y})) \quad (27)$$

$$= \mathbb{E}(\log p(\mathbf{Y} | \mathbf{X})) - D_{\text{KL}}(q(\mathbf{X} | \mathbf{Y}) \| p(\mathbf{X})). \quad (28)$$

The first term in equation 28 is an expected conditional likelihood that encourages  $q^*(\mathbf{X} | \mathbf{Y})$  to place mass on latent variables that explain the observed data well. The second term encourages densities close to the prior  $p(\mathbf{X})$ . The ELBO therefore encourages a balance between the conditional likelihood and the prior.

Finally, to see that the ELBO is a lower bound on the observed data likelihood, we can combine equations 25 and 26 to write

$$\log p(\mathbf{Y}) = D_{\text{KL}}(q(\mathbf{X} | \mathbf{Y}) \| p(\mathbf{X} | \mathbf{Y})) + \text{ELBO}(q). \quad (29)$$

Since the KL divergence is nonnegative, we have  $\log p(\mathbf{Y}) \geq \text{ELBO}(q)$  for any  $q(\mathbf{X} | \mathbf{Y})$ . Optimizing the ELBO therefore gives us two benefits at once: (1) It approximately maximizes the observed data likelihood, and (2) it drives  $q(\mathbf{X} | \mathbf{Y})$  to approximate the latent variable posterior  $p(\mathbf{X} | \mathbf{Y})$ .

### 4.3 The VAE Model

We now describe the *variational autoencoder* (VAE; Kingma & Welling, 2013; Rezende et al., 2014), an AE that performs approximate MLE by optimizing the ELBO. First, under fairly general distributional assumptions, the ELBO decomposes as a sum over observations (Hoffman, Blei, Wang, & Paisley, 2013):

$$\text{ELBO}(q) = \sum_{i=1}^N \left[ \mathbb{E}(\log p(\mathbf{y}_i | \mathbf{x}_i)) - D_{\text{KL}}(q(\mathbf{x}_i | \mathbf{y}_i) \| p(\mathbf{x}_i)) \right] \quad (30)$$

with expectations taken w.r.t.  $q(\mathbf{x}_i | \mathbf{y}_i)$ . This decomposition will allow us to optimize the ELBO using SGD.

Next, we specify each density in the ELBO. Following Kingma and Welling (2013), we specify the family of isotropic normal densities for the approximate latent variable posterior:

$$q(\mathbf{x}_i | \mathbf{y}_i) = \phi(\mathbf{x}_i | \boldsymbol{\mu}_i, \boldsymbol{\sigma}_i^2 \mathbf{I}), \quad (31)$$

where  $\boldsymbol{\mu}_i$  is a  $p \times 1$  mean vector for  $\mathbf{x}_i$ ,  $\boldsymbol{\sigma}_i^2$  is a  $p \times 1$  variance vector for  $\mathbf{x}_i$ , and  $\mathbf{I}$  is a  $p \times p$  identity matrix. Assuming the latent variables are uncorrelated, we specify a standard multivariate normal density for the latent variable prior:

$$p(\mathbf{x}_i) = \phi(\mathbf{x}_i | \mathbf{0}, \mathbf{I}), \quad (32)$$

where  $\mathbf{0}$  is a  $p \times 1$  zero mean vector and  $\mathbf{I}$  is a  $p \times p$  identity covariance matrix. We consider the more general case of correlated latent variables in Section 5.3. The form we choose for the observed variable conditional likelihood depends on

$\mathbf{y}_i$ . For example, if  $\mathbf{y}_i$  is dichotomous so that  $y_{i,j} \in \{0, 1\}$  for  $j = 1, \dots, n$ , we choose a factored Bernoulli density

$$p(\mathbf{y}_i | \mathbf{x}_i) = \prod_{j=1}^n \pi_{i,j}^{y_{i,j}} (1 - \pi_{i,j})^{(1-y_{i,j})}. \quad (33)$$

where  $0 \leq \pi_{i,j} \leq 1$  for all  $j$ .

The key idea of the VAE is to use an encoder FNN to parameterize  $q(\mathbf{x}_i | \mathbf{y}_i)$  and a decoder FNN to parameterize  $p(\mathbf{y}_i | \mathbf{x}_i)$  as follows:

$$\begin{aligned} (\boldsymbol{\mu}_i^\top, \log \boldsymbol{\sigma}_i^\top)^\top &= \text{EncoderFNN}(\mathbf{y}_i; \boldsymbol{\gamma}_1) \\ \boldsymbol{\pi}_i &= \text{DecoderFNN}(\mathbf{x}_i; \boldsymbol{\gamma}_2), \end{aligned} \quad (34)$$

where  $\boldsymbol{\mu}_i$  is a  $p \times 1$  predicted mean vector for  $\mathbf{x}_i$ ,  $\log \boldsymbol{\sigma}_i$  is a  $p \times 1$  predicted log-standard deviation vector for  $\mathbf{x}_i$ ,  $\boldsymbol{\pi}_i$  is an  $n \times 1$  predicted Bernoulli parameter vector for  $\mathbf{y}_i$ ,  $\boldsymbol{\gamma}_1$  is an  $r_1 \times 1$  parameter vector,  $\boldsymbol{\gamma}_2$  is an  $r_2 \times 1$  parameter vector,  $\text{EncoderFNN}(\cdot; \boldsymbol{\gamma}_1)$  is an FNN with  $L_1$  layers parameterized by  $\boldsymbol{\gamma}_1$ , and  $\text{DecoderFNN}(\cdot; \boldsymbol{\gamma}_2)$  is an FNN with  $L_2$  layers parameterized by  $\boldsymbol{\gamma}_2$ . VAEs are essentially AEs in which the prior ensures that the latent distribution is multivariate standard normal. Unlike AEs, however, VAEs are partly stochastic because we impute the factor scores  $\mathbf{x}_i$  by sampling from  $\phi(\mathbf{x}_i | \boldsymbol{\mu}_i, \boldsymbol{\sigma}_i^2 \mathbf{I})$ . Figure 3 visualizes a VAE with a single-layer encoder and a single-layer decoder.

#### 4.4 Optimizing the ELBO Using SGD

Fitting the VAE amounts to estimating the encoder and decoder FNN parameters  $\boldsymbol{\gamma} = (\boldsymbol{\gamma}_1^\top, \boldsymbol{\gamma}_2^\top)^\top$ . We now show how to estimate these parameters using SGD.

Let  $\text{ELBO}_i(q)$  denote the per-observation ELBO (i.e., a summand in equation 30). We must find an unbiased estimator for the gradient of  $\text{ELBO}_i(q)$  w.r.t. the FNN parameters. This is straightforward for the decoder parameters  $\boldsymbol{\gamma}_2$ :

$$\nabla_{\boldsymbol{\gamma}_2} \text{ELBO}_i(q) = \nabla_{\boldsymbol{\gamma}_2} \left( \mathbb{E}(\log p(\mathbf{y}_i | \mathbf{x}_i)) - D_{\text{KL}}(q(\mathbf{x}_i | \mathbf{y}_i) \| p(\mathbf{x}_i)) \right) \quad (35)$$

$$= \mathbb{E}(\nabla_{\boldsymbol{\gamma}_2} \log p(\mathbf{y}_i | \mathbf{x}_i)) \quad (36)$$

$$\approx \frac{1}{s} \sum_{k=1}^s \nabla_{\boldsymbol{\gamma}_2} \log p(\mathbf{y}_i | \mathbf{x}_{i,s}), \quad (37)$$

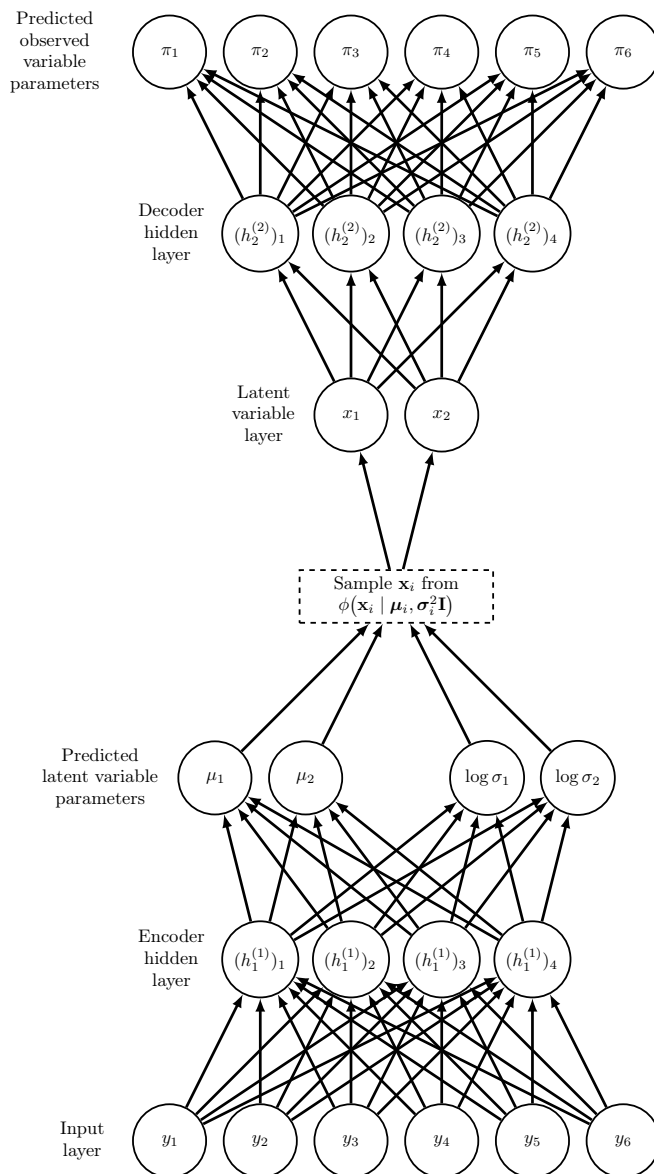
where line 37 approximates the expectation in line 36 using a size  $s$  Monte Carlo sample of factor scores from  $q(\mathbf{x}_i | \mathbf{y}_i)$ .

Finding an unbiased estimator of the gradient w.r.t. the encoder parameters  $\boldsymbol{\gamma}_1$  is less straightforward. This is because we sample from  $q(\mathbf{x}_i | \mathbf{y}_i)$  to impute the factor scores  $\mathbf{x}_i$ , but sampling is not differentiable. We can instead sample factor scores using a *reparameterization trick*:

$$\boldsymbol{\xi}_i \sim \phi(\boldsymbol{\xi}_i | \mathbf{0}, \mathbf{I}), \quad (38)$$

$$\mathbf{x}_i = \boldsymbol{\mu}_i + \boldsymbol{\sigma}_i \odot \boldsymbol{\xi}_i, \quad (39)$$

**Figure 3:** Schematic representation of a variational autoencoder with a single-layer encoder and a single-layer decoder.



where  $\boldsymbol{\xi}_i$  is a  $p \times 1$  sample from a standard multivariate normal density for observation  $i$  and  $\odot$  denotes element-wise multiplication. The sampled  $\mathbf{x}_i$  is now differentiable w.r.t.  $\boldsymbol{\gamma}_2$  because  $\boldsymbol{\gamma}_2$  is removed from the sampling step.

We now have an unbiased estimator for the gradient of the per-observation ELBO w.r.t. the FNN parameters  $\boldsymbol{\gamma}$ :

$$\begin{aligned} \nabla_{\boldsymbol{\gamma}} \text{ELBO}_i(q) = \nabla_{\boldsymbol{\gamma}} \left[ \frac{1}{s} \sum_{k=1}^s \log p(\mathbf{y}_i \mid \boldsymbol{\mu}_i + \boldsymbol{\sigma}_i^2 \odot \boldsymbol{\xi}_{i,s}) \right. \\ \left. - D_{\text{KL}}(q(\mathbf{x}_i \mid \mathbf{y}_i) \parallel p(\mathbf{x}_i)) \right]. \end{aligned} \quad (40)$$

In practice, we set Monte Carlo sample size  $s = 1$ . Also notice that when the latent variable posterior is isotropic normal and the latent variable prior is standard multivariate normal, the per-observation KL divergence has a closed form that is efficient to optimize:

$$-D_{\text{KL}}(q(\mathbf{x}_i \mid \mathbf{y}_i) \parallel p(\mathbf{x}_i)) = \frac{1}{2} \sum_{t=1}^p \left[ 1 + \log \sigma_{i,t}^2 - \sigma_{i,t}^2 - \mu_{i,t}^2 \right], \quad (41)$$

where  $\mu_{i,t}$  is the  $t^{\text{th}}$  element of the  $p \times 1$  mean vector  $\boldsymbol{\mu}_i$  and  $\sigma_{i,t}^2$  is the  $t^{\text{th}}$  element of the  $p \times 1$  variance vector  $\boldsymbol{\sigma}_i^2$ .

## 5 VAEs for Exploratory IFA

### 5.1 Fitting the GRM

Fitting the GRM requires a VAE with a specific decoder FNN and a specific observed data conditional likelihood. We give these specifications below.

We output the GRM boundary response probabilities in equation 1 from a decoder FNN with a specific regression weight matrix. Let  $\mathbf{P}_i = (\mathbf{P}_{i,1}^\top, \mathbf{P}_{i,2}^\top, \dots, \mathbf{P}_{i,n}^\top)^\top$  denote the  $(\sum_{j=1}^n (C_j - 1)) \times 1$  vector of boundary response probabilities for respondent  $i$  where  $\mathbf{P}_{i,j} = (P_{i,j,1}, P_{i,j,2}, \dots, P_{i,j,C_j-1})^\top$  denotes the  $(C_j - 1) \times 1$  vector of boundary response probabilities for  $y_{i,j}$ . Let  $\boldsymbol{\alpha} = (\boldsymbol{\alpha}_1^\top, \boldsymbol{\alpha}_2^\top, \dots, \boldsymbol{\alpha}_p^\top)^\top$  be a vector collecting the intercept parameters for all items. Let  $\boldsymbol{\beta}$  denote the  $n \times p$  loadings matrix whose  $j^{\text{th}}$  row is  $\boldsymbol{\beta}_j^\top$ . Let  $\mathbf{1}_j$  and  $\mathbf{0}_j$  denote  $(C_j - 1) \times 1$  vectors of ones and zeros, respectively. We parameterize  $\mathbf{P}_i$  with a decoder FNN as

$$\mathbf{P}_i = \text{DecoderFNN}(\mathbf{x}_i; \boldsymbol{\gamma}_2) = \psi(-\mathbf{D}\boldsymbol{\beta}\mathbf{x}_i - \boldsymbol{\alpha}), \quad (42)$$

where

$$\mathbf{D} = \begin{bmatrix} \mathbf{1}_1 & \mathbf{0}_1 & \cdots & \mathbf{0}_1 \\ \mathbf{0}_2 & \mathbf{1}_2 & \cdots & \mathbf{0}_2 \\ \vdots & \vdots & \ddots & \vdots \\ \mathbf{0}_n & \mathbf{0}_n & \cdots & \mathbf{1}_n \end{bmatrix} \quad (43)$$

is a  $(\sum_{j=1}^n (C_j - 1)) \times n$  block diagonal matrix with vectors of ones on the diagonal and zeros elsewhere and  $\psi(\cdot)$  is the inverse logit activation function. Note that the decoder in Curi et al.’s 2019 VAE for M2PL IFA is a special case of equation 42 where  $\mathbf{D}$  is an  $n \times n$  identity matrix.

Our VAE for fitting the GRM is fully specified by setting the observed data conditional likelihood  $p(\mathbf{y}_i | \mathbf{x}_i)$  to the form in equation 5. Notice we place no restrictions on our VAE encoder FNN, which may be any deep FNN. This corresponds to non-linear factor score estimation and allows the model to capture complicated relationships between the observed and latent variables.

## 5.2 Regularized Exploratory IFA

We now show how to conduct exploratory IFA with our VAE for fitting the GRM. While traditional approaches to exploratory factor analysis (EFA) rely on an additional factor rotation step after fitting (Browne, 2001), our approach relies on developments in regularized EFA that produce interpretable models by penalizing factor loadings directly during fitting (Scharf & Nestler, 2019; Trendafilov, 2014; Yamamoto, Hirose, & Nagata, 2017).

The key idea of regularized EFA is to add a penalty term to the objective function to encourage sparsity in the factor loadings matrix. In this paper, we place a *lasso* penalty (Tibshirani, 1996) on the loadings matrix as follows:

$$- \text{ELBO}(q) + \lambda \|\boldsymbol{\beta}\|_1, \quad (44)$$

where  $\lambda \in \mathbb{R}_+$  is the *regularization hyperparameter*. As  $\lambda$  increases, the penalized parameters shrink toward or all the way to zero. Importantly, setting  $\lambda > 0$  removes the rotational indeterminacy of traditional EFA so that the loadings estimates are unique up to a re-ordering of factors or to loadings sign changes (Choi, Oehlert, & Zou, 2010; Scharf & Nestler, 2019).

We optimize equation 44 using *proximal SGD* (Parikh, 2013), an approach to optimization problems of the form

$$\arg \min_{\boldsymbol{\gamma}} J(\boldsymbol{\gamma}) + \Omega(\boldsymbol{\gamma}), \quad (45)$$

where  $\boldsymbol{\gamma}$  is an  $r \times 1$  parameter vector,  $J(\boldsymbol{\gamma})$  is smooth but possibly non-convex, and  $\Omega(\boldsymbol{\gamma})$  is non-smooth but convex. Proximal mini-batch SGD first performs one iteration of mini-batch SGD on  $J(\boldsymbol{\gamma})$  following equation 18, then takes a corrective *proximal step* w.r.t.  $\Omega(\boldsymbol{\gamma})$ . When  $\Omega(\boldsymbol{\gamma})$  is a lasso penalty, the proximal step updates  $\boldsymbol{\gamma}$  at each iteration as

$$\gamma_{j,k+1} = \frac{\gamma_{j,k}}{|\gamma_{j,k}|} \max(0, |\gamma_{j,k}| - \nu\lambda), \quad (46)$$

where  $\gamma_{j,k}$  is the  $j^{\text{th}}$  element of  $\boldsymbol{\gamma}$  at iteration  $k$  for  $j = 1, \dots, r$  and  $\nu \in \mathbb{R}_+$  is the *proximal step size*. Alternating mini-batch SGD steps followed by corrective proximal steps continue until  $\boldsymbol{\gamma}$  converges to a stationary point, which is guaranteed under certain conditions (Reddi, Sra, Póczos, & Smola, 2016).

### 5.3 Correlated Factors

Previously, we assumed that the factors were uncorrelated by placing a standard normal prior on the factor scores (equation 32). In general, however, uncorrelated factors may be hard to justify theoretically. Additionally, allowing correlated factors may reduce the need for cross-loadings that make the factor structure less interpretable. We now show how to allow for correlated factors by estimating the factor covariance matrix. Choosing either correlated or uncorrelated factors using our approach corresponds to choosing either oblique or orthogonal rotation in traditional EFA, respectively.

Assume the factors are mean-centered and multivariate normally distributed:

$$p(\mathbf{x}_i) = \phi(\mathbf{x}_i \mid \mathbf{0}, \mathbf{\Sigma}). \quad (47)$$

Equation 47 modifies the prior in equation 32 by allowing for factor inter-correlations. Our goal is to estimate  $\mathbf{\Sigma}$ . We first decompose  $\mathbf{\Sigma}$  as

$$\mathbf{\Sigma} = \mathbf{L}\mathbf{L}^\top, \quad (48)$$

where  $\mathbf{L} \in \mathbb{R}^{p \times p}$  is the lower-triangular *Cholesky decomposition* of  $\mathbf{\Sigma}$ , which is estimable without constrained optimization (Pinheiro & Bates, 1996). Next, notice that the prior only appears in the ELBO in the KL divergence term (equation 30). We can re-write the negative single-observation KL divergence as

$$-D_{\text{KL}}(q(\mathbf{x}_i \mid \mathbf{y}_i) \parallel p(\mathbf{x}_i)) = \mathbb{E}(\log p(\mathbf{x}_i)) - \mathbb{E}(\log q(\mathbf{x}_i \mid \mathbf{y}_i)) \quad (49)$$

$$\approx \frac{1}{s} \sum_{k=1}^s \left[ \log p(\mathbf{x}_{i,k}) - \log q(\mathbf{x}_{i,k} \mid \mathbf{y}_i) \right], \quad (50)$$

where line 50 is a Monte Carlo approximation to the expectations in line 49. The prior and posterior log-densities have the closed forms

$$\log p(\mathbf{x}_{i,k}) = -\frac{1}{2} \sum_{t=1}^p \left[ \log 2\pi + 2 \log |l_{t,t}| \right] - \frac{1}{2} \mathbf{x}_{i,k}^\top (\mathbf{L}^{-1})^\top \mathbf{L}^{-1} \mathbf{x}_{i,k} \quad (51)$$

and

$$\log q(\mathbf{x}_{i,k} \mid \mathbf{y}_i) = - \sum_{t=1}^p \left[ \frac{1}{2} \xi_{i,t,k}^2 + \frac{1}{2} \log 2\pi - \log \sigma_{i,t} \right], \quad (52)$$

respectively, where  $x_{i,t,k}$  is the  $t^{\text{th}}$  element of  $\mathbf{x}_{i,k}$ ,  $|l_{t,t}|$  are the absolute values of the diagonal elements of  $\mathbf{L}$ , and  $\xi_{i,t,k}$  is the  $t^{\text{th}}$  element of the random noise vector  $\boldsymbol{\xi}_{i,k}$  (equation 39) for Monte Carlo sample  $k = 1, \dots, s$ . As before, we set  $s = 1$  in practice.  $\mathbf{L}$  is now estimable using mini-batch SGD.

### 5.4 Starting Values, Stabilizing Fitting, and Checking Convergence

We now discuss practical strategies for model fitting. Our empirical examples include multiple random starts to assess these strategies across random seeds.

For the encoder FNN, we initialize a  $p_l \times p_{l-1}$  regression weight matrix  $\mathbf{W}^{(l)}$  and a  $p_l \times 1$  intercept vector  $\mathbf{b}^{(l)}$  at each layer  $l \in \{1, \dots, L_1\}$ . We use an initialization strategy that has demonstrated good performance when applied to ANNs with ReLU activation functions (He, Zhang, Ren, & Sun, 2015). Let  $\mathcal{U}(a, b)$  denote a uniform density with lower bound  $a$  and upper bound  $b$ . We randomly sample starting values as

$$w_{j,k}^{(l)}, b_j^{(l)} \sim \mathcal{U}\left(-\frac{1}{\sqrt{p_l}}, \frac{1}{\sqrt{p_l}}\right) \quad (53)$$

for  $j = 1, \dots, p_l$ ,  $k = 1, \dots, p_{l-1}$ ,  $l = 1, \dots, L$ . This often prevents the  $\mathbf{W}^{(l)} \mathbf{h}_i^{(l-1)} + \mathbf{b}^{(l)}$  values from growing too large or too small at the start of fitting while accounting for the asymmetry of ReLU about the origin.

For the decoder FNN, we initialize the  $p(p+1)/2$  elements of the Cholesky decomposition  $\mathbf{L}$  of the factor covariance matrix, the  $n \times p$  loadings matrix  $\beta$ , and the  $(\sum_{j=1}^n (C_j - 1)) \times 1$  vector of intercepts for all items  $\alpha = (\alpha_1^\top, \alpha_2^\top, \dots, \alpha_p^\top)^\top$ . We draw the elements of  $\mathbf{L}$  from a standard normal distribution. We initialize loadings to one so that proximal mini-batch SGD does not quickly take too many estimates to zero. For  $k = 1, \dots, p$ , we initialize the elements of  $\alpha_k$  to an increasing sequence such that the cumulative density of logistic distribution between consecutive elements is the same (Christensen, 2019).

We use *KL annealing* to avoid entrapment in sub-optimal local stationary points at the start of fitting (Bowman et al., 2016; Kingma et al., 2016; Sønderby, Raiko, Maaløe, Sønderby, & Winther, 2016). KL annealing multiplies the per-observation KL divergences by  $\frac{k-1}{M}$  for the first  $M$  mini-batches where  $k = 1, \dots, M$ . We conduct KL annealing for  $M = 1,000$  mini-batches for all models. We also stabilize fitting by setting loadings estimates to  $\max(0, \beta_{j,k})$  during KL annealing to avoid initial loadings sign oscillations.

We monitor convergence by plotting the ELBO as a function of fitting iteration (i.e., epoch) and waiting until the plot levels off. Fitting is terminated when the ELBO converges after KL annealing. Note that evaluating models by visually monitoring the objective function over fitting iterations is subjective but performs well in DL research (Bengio, 2012; Smith, 2018).

## 5.5 Hyperparameter Tuning

Hyperparameters for our model include the number and size of the encoder FNN hidden layers, the learning rate  $\eta_k$ , the proximal step size  $\nu$ , the mini-batch size  $m$ , and the regularization hyperparameter  $\lambda$ . All hyperparameters except  $\lambda$  require little to no tuning if chosen reasonably.

We experimented with the number and size of the encoder FNN hidden layers but found that model performance was relatively insensitive to these values. We therefore use a single hidden layer for all models and set the hidden layer size to a value close to the mean of the input layer size and the number of factors. We set the initial learning rate  $\eta_0$  and the proximal step size  $\nu$  to  $1^{-3}$  for all analyses. For each SGD step, we employ an “adaptive” learning rate following



Reddi, Kale, and Kumar (2018) where  $\eta_k$  is scaled by square roots of exponential moving averages of squared past gradients. This approach is called AMSGrad and is implemented in several major deep learning libraries. We set  $m$  to 128 for all analyses. These hyperparameter values are specified based on recommended default values that perform well in practice (e.g., Bengio, 2012; Heaton, 2008).

Model performance was most sensitive to the regularization hyperparameter  $\lambda$ . To choose  $\lambda$ , we conducted 5-fold cross-validation (CV) for a range of  $\lambda$  values to obtain a cross-validated ELBO for each value. Since higher ELBOs indicate better model fit, we chose the  $\lambda$  corresponding to the sparsest and most theoretically justified model within some neighborhood of the model with the highest cross-validated ELBO. Typically, the chosen model’s cross-validated ELBO was within one standard error (e.g., McNeish, 2015) or within one percent (Knafl & Grey, 2010) of the highest cross-validated ELBO.

## 6 Numerical Illustrations

In this section, we first examine our algorithm’s performance in two large empirical examples. We then conduct two simulation studies based on our empirical results. Loadings and intercepts are presented in the normal metric following Cai (2010b), which corresponds to setting the scaling factor  $D = 1.702$  in equation 1. Models were programmed with the machine learning library PyTorch (Version 1.1.0; Paszke et al., 2017) and were fitted on a laptop computer with a 2.8 GHz Intel Core i7 CPU and 16 GB of RAM. Although GPU computing is directly supported in PyTorch and may have sped up model fitting, we opted for CPU computing to assess performance using hardware more typically employed in psychology and education research settings.

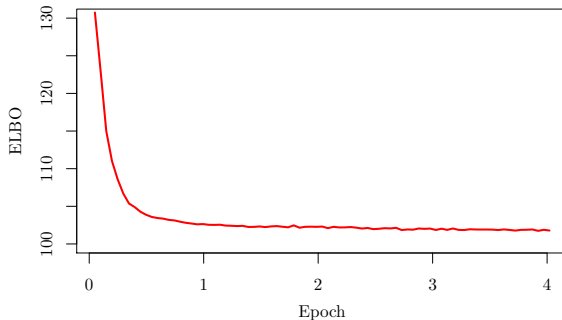
### 6.1 Empirical Examples

#### 6.1.1 A Big-Five Personality Factors Data Set

Data were 1,015,342 responses to Goldberg’s (1992) 50 Big-Five Factor Marker (FFM) items from the International Personality Item Pool (IPIP; Goldberg et al., 2006) downloaded from the Open-Source Psychometrics Project (<https://openpsychometrics.org/>). The IPIP-FFM items were designed to assess respondents’ levels of five personality factors: *Conscientiousness*, *openness*, *emotional stability*, *agreeableness*, and *extraversion*. Empirical Big-Five studies often yield substantial factor inter-correlations (e.g., Biesanz & West, 2004), so we permitted correlated factors during fitting. Each of the five factors included 10 five-category items anchored by “Disagree” (1), “Neutral” (3), and “Agree” (5). Item responses were recoded as necessary so that the highest numerical value of the response scale indicated a high level of the corresponding factor.

To pre-process the data, we first dropped 318,496 responses with multiple submissions from the same IP address to reduce the chances of including the same respondent multiple times. Although VAEs can be fitted with incomplete data (e.g., Nazabal, Olmos, Ghahramani, & Valera, 2018), we dropped 93,523

**Figure 4:** Plot of negative mean per-observation ELBO as a function of fitting epoch (i.e., number of passes through the full data set) for IPIP-FFM data set.



responses with missing values to simplify the data example. We then dropped 87,615 careless responses based on four indicators: LongString, survey time, number of Guttman errors, and Mahalanobis distance (details available upon request). These indicators have demonstrated good sensitivity and specificity with simulated data (Desimone, Harms, & Desimone, 2015; Meade & Craig, 2012; Niessen, Meijer, & Tendeiro, 2016). Our final sample size was  $N = 515,708$  responses.

Our encoder FNN had one hidden layer of size 30. After 5-fold CV, we set  $\lambda = 3$  which produced a model whose cross-validated ELBO (ELBO =  $-10,617,610$ ;  $SE = 2,275$ ) was within one percent of the largest cross-validated ELBO (ELBO =  $-10,575,444$ ;  $SE = 1,058$ ). We monitored the ELBO for a random 2.5 percent of observations because computing the ELBO for the full sample was prohibitively time-intensive. The ELBO plot leveled off after one epoch (i.e., one full pass through the data set; Figure 4). Fitting the entire data set took 4 minutes and 26 seconds. Table 1 contains the loadings obtained from our fitted model, which generally fit with the expected five factor structure. Factor correlations in Table 2 also fit with the typical finding that emotional stability is negatively correlated with the other factors.

We also assessed whether estimates were consistent across random seeds. Although loadings estimates at equivalent ELBOs are rotation invariant due to the lasso penalty, different starting values may re-order the loadings matrix columns. We therefore compared loadings matrices across starting values by selecting a reference loadings matrix and finding the column permutation of each comparison matrix that minimized the element-wise MSE. Factors were inverted before being compared if the sum of their loadings was negative (Scharf & Nestler, 2019). Across 100 sets of random starting values, mean column-permuted RMSE for loadings was 0.03 ( $SD = 0.02$ ) and mean RMSE for intercepts was 0.07 ( $SD = 0.02$ ), which are small relative to primary loadings and intercept magnitudes and would not meaningfully change the conclusions of the analysis.

**Table 1:** Factor Loadings for IPIP-FFM Big-Five Factor Marker Items

Item	Factor				
	1	2	3	4	5
Conscientiousness					
1	<b>.52</b>	.06	-.01	.01	.02
2	<b>.54</b>	-.03	-.01	-.04	-.03
3	<b>.34</b>	.30	.02	.06	-.03
4	<b>.52</b>	.04	-.21	.03	.01
5	<b>.54</b>	-.07	-.01	.01	.05
6	<b>.62</b>	-.02	-.02	-.03	.00
7	<b>.51</b>	.07	.13	.02	.01
8	<b>.41</b>	.09	-.09	.11	.01
9	<b>.54</b>	-.02	.08	.05	.05
10	<b>.33</b>	.29	.02	.02	.00
Openness					
1	.03	<b>.55</b>	.00	-.06	-.02
2	-.01	<b>.64</b>	-.11	.00	-.01
3	-.06	<b>.59</b>	.09	.06	.00
4	-.07	<b>.60</b>	-.06	.02	-.06
5	.06	<b>.59</b>	-.01	-.03	.10
6	-.04	<b>.61</b>	-.02	.07	.02
7	.11	<b>.52</b>	-.10	-.01	.01
8	-.01	<b>.48</b>	.04	-.11	-.01
9	.02	<b>.47</b>	.05	.15	-.11
10	-.03	<b>.69</b>	.01	.00	.05
Emotional Stability					
1	.07	.00	<b>.59</b>	.11	-.03
2	.11	.00	<b>.48</b>	.01	-.01
3	.08	.08	<b>.50</b>	.22	-.09
4	.00	.10	<b>.36</b>	.03	-.09
5	-.01	-.04	<b>.41</b>	-.01	.00
6	.00	-.02	<b>.64</b>	.02	.02
7	-.05	.01	<b>.61</b>	.01	.07
8	-.05	-.01	<b>.66</b>	-.04	.06
9	.04	.01	<b>.59</b>	-.09	.03
10	-.07	.07	<b>.52</b>	-.01	-.14
Agreeableness					
1	.00	.00	.00	<b>.56</b>	-.03
2	.00	.03	-.04	<b>.51</b>	.21
3	.10	-.01	-.16	<b>.34</b>	-.13
4	-.01	.00	.04	<b>.74</b>	-.07
5	-.01	-.02	.00	<b>.63</b>	.02
6	.00	-.03	.10	<b>.53</b>	-.05
7	.00	.00	-.06	<b>.61</b>	.17
8	.04	-.01	-.02	<b>.51</b>	.03
9	.00	.02	.06	<b>.64</b>	.00
10	.03	.05	-.09	<b>.35</b>	.17
Extraversion					
1	-.05	-.04	.01	-.01	<b>.57</b>
2	.01	.01	.07	.05	<b>.60</b>
3	.04	-.04	-.17	.16	<b>.50</b>
4	.01	.00	-.01	-.01	<b>.62</b>
5	.04	.03	-.01	.13	<b>.59</b>
6	.01	.29	.00	.08	<b>.42</b>
7	.00	-.02	.00	.05	<b>.63</b>
8	-.04	-.01	.03	-.12	<b>.53</b>
9	-.03	.10	-.01	-.07	<b>.54</b>
10	-.01	-.07	-.02	-.04	<b>.60</b>

*Note.* Highest loading for each item is bold.

**Table 2:** Factor Correlations for IPIP-FFM Big-Five Factor Marker Items

Factor	Factor				
	1	2	3	4	5
1. Conscientiousness	1.00				
2. Openness	.07	1.00			
3. Emotional Stability	-.28	-.10	1.00		
4. Agreeableness	.14	.53	-.07	1.00	
5. Extraversion	.01	.03	-.25	.15	1.00

### 6.1.2 A Drug Use and Mental Health Data Set

Data were 56,276 responses to  $n = 218$  substance use and mental health items from the 2017 National Survey on Drug Use and Health (NSDUH) downloaded from the Substance Abuse and Mental Health Data Archive (SAMHSA; <https://www.datafiles.samhsa.gov/>). Items were designed to measure *dependence on nicotine, dependence and abuse of illicit drugs and alcohol, non-specific psychological distress, functional impairment* (FI; i.e., disturbances in social adjustment and behavior), and *major depression*. We summarize the subscales used in Table 3. Details on subscale development and item wording are given in the 2017 NSDUH Codebook (Center for Behavioral Health Statistics and Quality, 2018a). Responses were recoded as necessary so that the highest numerical response value indicated a high level of the corresponding factor.

We pre-processed the data by first dropping 13,722 respondents aged 18 or younger because these respondents were not administered all of the subscales in Table 3. Missing item responses were imputed with the smallest numerical response value as recommended the 2017 NSDUH Methodological Summary and Definitions (Center for Behavioral Health Statistics and Quality, 2018b) to ensure that our estimates were comparable with estimates derived using NSDUH data from previous years. The NSDUH was administered during interviews in respondents’ homes rather than as a web-based survey, so we did not screen for careless responses. Our final sample size was  $N = 42,526$  responses.

Our encoder FNN had one hidden layer of size 75. We initially fitted models with up to 27 factors (i.e., the number of factors in Table 3) but consistently found that the lasso pruned all but four columns from the loadings matrix. We therefore set  $p = 4$  factors for all analyses. 5-fold CV failed to produce a sparse model whose cross-validated ELBO was within one percent of the largest cross-validated ELBO (ELBO =  $-365,432$ ;  $SE = 1,678$ ). We therefore set  $\lambda = 3$ , which was the smallest  $\lambda$  that produced a sparse, theoretically reasonable model (ELBO =  $-398,784$ ;  $SE = 3,661$ ). The ELBO plot for a random 10 percent of observations leveled off at 6 epochs. Fitting took 3 minutes and 33 seconds.

We present a heat map of loadings estimates in Figure 5. The model recovered an incomplete bifactor structure where all items loaded on the general factor, the major depressive episode (MDE) items loaded on the first specific factor, the psychological distress and general FI items loaded on the second specific factor, and the nicotine dependence items loaded on the third specific factor. The MDE-related FI items also cross-loaded on the psychological distress and FI

**Table 3:** Summary of 2017 NSDUH Substance Use and Mental Health Subscales

Subscale	Factor	No. Items	No. Response Categories	
NDSS	Nicotine Dependence	17	5	
DSM-IV Dependence Criteria	Alcohol Dependence	10	2	
	Marijuana Dependence	9	2	
	Cocaine Dependence	11	2	
	Heroin Dependence	10	2	
	Hallucinogen Dependence	9	2	
	Inhalant Dependence	9	2	
	Meth. Dependence	11	2	
	Pain Reliever Dependence	10	2	
	Tranquilizer Dependence	9	2	
	Stimulant Dependence	10	2	
	Sedative Dependence	10	2	
	DSM-IV Abuse Criteria	Alcohol Abuse	5	2
		Marijuana Abuse	5	2
		Cocaine Abuse	5	2
Heroin Abuse		5	2	
Hallucinogen Abuse		5	2	
Inhalant Abuse		5	2	
Meth. Abuse		5	2	
Pain Reliever Abuse		5	2	
Tranquilizer Abuse		5	2	
Stimulant Abuse		5	2	
Sedative Abuse		5	2	
K6 Psychological Distress Scale		Psychological Distress	6	5
WHODAS		General FI	8	4
DSM-5 MDE Criteria		MDE	20	2
SDS	MDE-Related FI	4	11	

*Note.* NDSS = Nicotine Dependence Syndrome Scale; DSM = Diagnostic Statistical Manual; Meth. = Methamphetamine; WHODAS = World Health Organization Disability Assessment Schedule; MDE = Major Depressive Episode; SDS = Sheehan Disability Scale; FI = function impairment.

specific factor. This is likely because the MDE-related FI items (e.g., “During the time in the past 12 months when your depression symptoms were most severe, how much did this interfere with your ability to work?”) were similar to the general FI items (e.g., “During that one month when your emotions, nerves or mental health interfered most with your daily activities, how much difficulty did you have taking care of your daily responsibilities at work or school?”) – that is, this factor captured the correlations between items measuring FI. Our VAE recovered the incomplete bifactor structure when fitted with and without correlated factors, so we disallowed correlated factors in the final model in accordance with how bifactor models are typically specified (Reise, 2012).

Our results align theoretically with recent findings that a general “transdiagnostic” factor as well as several specific factors often underlie psychopathology symptom data (e.g., Chen, Yoon, Harford, & Grant, 2017; Reininghaus et al., 2016; Shevlin, McElroy, Bentall, Reininghaus, & Murphy, 2017). However, traditional confirmatory approaches to bifactor analysis are unlikely to arrive at the complex factor structure uncovered here. For example, our approach lets items load on more than one specific factor, whereas most bifactor structures assume each item is affected by at most one specific factor. The number of items

considered here also exceeds what is typical for a bifactor application conducted using conventional estimation approaches.

We assessed parameter estimate consistency across different random starting values using the column-permutation approach described previously. As before, we only compared estimates at equivalent ELBOs. Across 100 sets of random starting values, mean column-permuted RMSE for loadings was 0.02 ( $SD = 0.02$ ) and mean RMSE for intercepts was 0.04 ( $SD = 0.02$ ), which are small relative to primary loadings and intercept magnitudes.

## 6.2 Simulation Studies

### 6.2.1 A Simple Factor Pattern

Our first simulation aimed to firmly establish proof of concept by verifying our VAE’s ability to recover loadings and intercept parameters in the case of simple factor structure. We also aimed to demonstrate that parameter recovery is feasible even with a moderate sample size.

The data generating IFA model had  $p = 5$  factors and  $n = 50$  five-category items. Generating parameters were chosen by rounding the estimates recovered for the IPIP-FFM data set (details available upon request). All cross loadings were set to zero to produce a simple factor structure. We set the sample size to  $N = 2,000$ , which is reasonable for Big-Five personality factor samples (van der Linden, te Nijenhuis, & Bakker, 2010) but is still fairly large for many psychology and education research areas. We conducted 100 replications to explore the impact of sampling variability on parameter estimates.

We fitted a VAE with an encoder FNN hidden layer size of 30 and with correlated factors. We set  $\lambda = 2$  after 5-fold CV to obtain a cross-validated ELBO (ELBO =  $-44,209$ ;  $SE = 80$ ) within one standard error of the largest cross-validated ELBO (ELBO =  $-44,178$ ;  $SE = 84$ ). We determined the number of epochs required for convergence by fitting the model with a single simulated data set. The ELBO plot for this data set leveled off after 400 epochs, so we fitted each replication for 400 epochs. Mean fitting time across replications was 3 minutes and 53 seconds ( $SD = 6$  seconds).

We calculated summary statistics at each replication. Tucker’s congruence coefficient averaged across factors was used as a measure of similarity between true and estimated loadings (Lorenzo-Seva & ten Berge, 2006). Mean bias was calculated separately for primary loadings, cross loadings, and intercepts to measure parameter recovery. Following previous studies (e.g., Asparouhov & Muthén, 2009; Scharf & Nestler, 2019), we defined mean bias as the average deviation of the estimated parameters from the data generating parameters.

Table 4 contains Monte Carlo averages and standard deviations of all summary statistics. Tucker’s congruence coefficient consistently achieved its maximum value of 1.00 and primary loadings as well as cross loadings were unbiased across replications, indicating excellent recovery of the true loadings. The model consistently overestimated intercepts by a small amount.

**Figure 5:** Heat map of factor loadings for 2017 NSDUH substance use and mental health items.

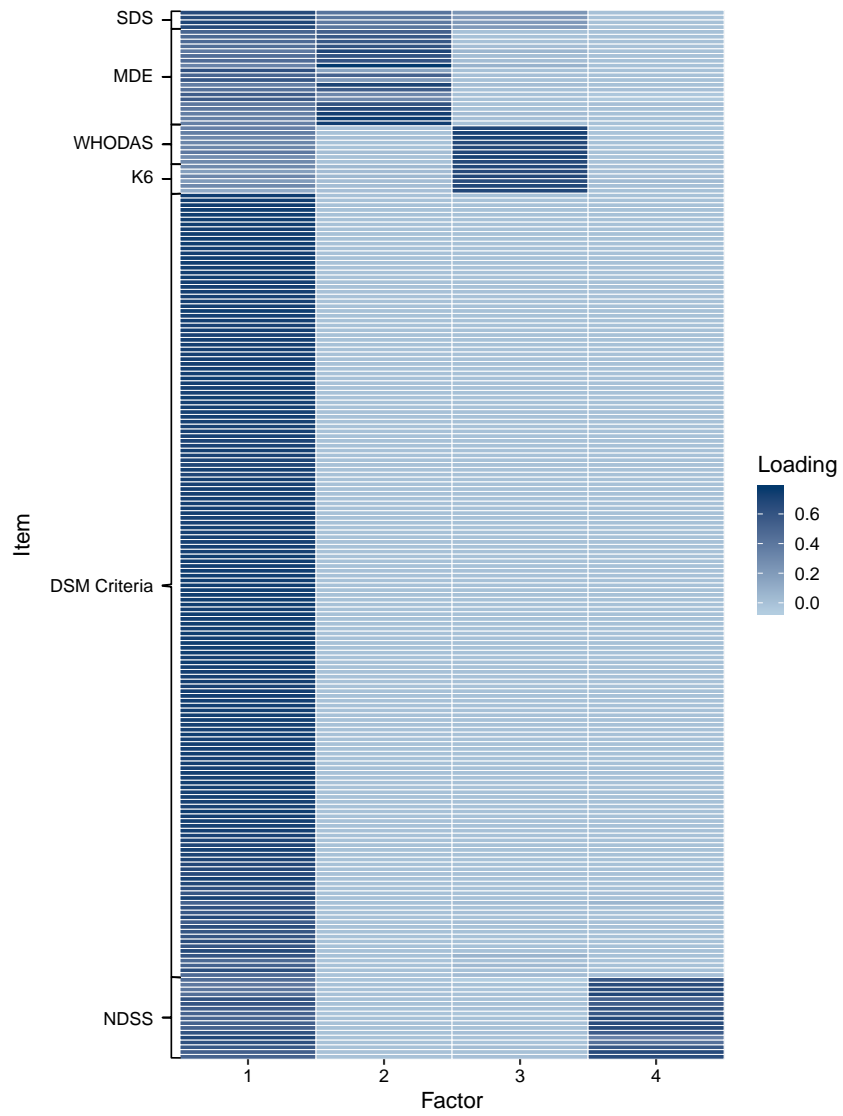


**Table 4:** Congruence Coefficients and Mean Biases for Simulation Studies

Measure	Condition	
	Simple Structure	Incomplete Bifactor
Congruence Coefficient	1.00 (.00)	.98 (.04)
Primary Loadings Mean Bias	.00 (.00)	.00 (.03)
Secondary Loadings Mean Bias		-.19 (.01)
Cross Loadings Mean Bias	.00 (.00)	.00 (.01)
Intercepts Mean Bias	.07 (.01)	-.10 (.00)

*Note.* All summary statistics are Monte Carlo averages; Monte Carlo standard deviations are in parentheses.

### 6.2.2 An Incomplete Bifactor Pattern

Our second simulation aimed to explore parameter recovery with a complex factor pattern and a large number of items. The data generating IFA model had  $p = 4$  factors and  $n = 218$  two- to eleven-category items. IFA model parameters were chosen by rounding the estimates recovered for the NSDUH data set and small cross loadings were set to zero to produce an incomplete bifactor structure with three specific factors (details available upon request). We again set the sample size to  $N = 2,000$  and conducted 100 replications.

Our VAE encoder FNN had a hidden layer of size 75 and factors were uncorrelated. We set  $\lambda = 1$  after 5-fold CV to obtain a cross-validated ELBO (ELBO =  $-99,347$ ;  $SE = 512$ ) equal to largest cross-validated ELBO (ELBO =  $-99,347$ ;  $SE = 485$ ). The ELBO plot for a single data set leveled off after 200 epochs, so all replications were fitted for 200 epochs. Mean fitting time was 4 minutes and 23 seconds ( $SD = 8$  seconds).

Monte Carlo averages and standard deviations of summary statistics are in Table 4. High values for Tucker’s congruence coefficient and unbiased cross loadings estimates suggest that factor pattern recovery was consistently excellent. Since many items loaded on two factors, we calculated mean bias separately for primary and secondary loadings (i.e., larger and smaller true loadings, respectively). Primary loadings estimates were unbiased but secondary loadings were consistently underestimated. This result aligns with Scharf and Nestler’s (2019) finding that lasso underestimates smaller loadings when items load on multiple factors. Intercepts were moderately underestimated across replications.

## 7 Discussion

In this paper, we demonstrated connections between a DL model called the variational autoencoder and multidimensional item factor analysis. We combined the VAE with a regularization technique to fit high-dimensional exploratory IFA models to both real and simulated data sets. Our empirical analyses yielded



factor patterns that aligned with existing psychological theory in both a Big-Five personality factors data set and in a more complicated psychopathology symptoms data set. Our simulations suggested that the regularized VAE consistently recovers the data generating factor pattern and accurately recovers all loadings in the case of simple structure. Notably, fitting was fast compared to traditional methods: All models converged in minutes, even with hundreds of thousands of observations, hundreds of items, and up to 27 factors. However, “big data” was not *required* for convergence, and factor pattern recovery was excellent even with moderate-sized data sets ( $N = 2,000$ ). Additionally, fitting was not overly complicated: Only the regularization hyperparameter required significant tuning.

Despite the regularized VAE’s promising performance, the method has several limitations. First, secondary loadings were underestimated in the incomplete bifactor simulation study and intercept estimates were moderately biased in both simulation studies. The secondary loadings estimate bias is likely due to the lasso penalty’s tendency to over-shrink smaller loadings when items load on multiple factors (Scharf & Nestler, 2019) and may be alleviated by using a different regularization penalty (e.g., Yamamoto et al., 2017). It is unclear to what extent the intercept estimate bias is due to (1) inaccurate loadings estimates due to the lasso penalty, (2) insufficient sample size, or (3) the approximate nature of the ELBO. Future work may investigate these problems further.

Second, our convergence criteria were subjective. Subjective convergence criteria are typical in DL, where researchers focus on performance metrics like accuracy or likelihood and rarely discuss how convergence was established. The DL literature does include objective techniques for checking convergence (e.g., Prechelt, 2012), but these techniques were prohibitively time-intensive for our models. Our model selection criteria were also subjective. Although  $k$ -fold cross validation is a popular model selection approach in psychology and in education, it often failed to select sparse models in our empirical analyses. Future work should explore objective convergence and model selection criteria to help automate model fitting and specification.

Third, obtaining standard errors (SEs) for our parameter estimates is non-trivial. Obtaining SEs via bootstrap would be straightforward but computationally intensive when each model takes several minutes to fit. Approaches that compute SEs for SGD by accumulating variability information during fitting typically assume that the objective function is convex (e.g., Fang, Xu, & Yang, 2018). It is challenging to derive guarantees about the statistical properties of estimators obtained using variational approximations (Westling & McCormick, 2019). Additionally, computing SEs for regularized models is difficult because naive SEs fail account for the uncertainty of tuning the regularization hyperparameter. We leave the necessary theoretical developments to future research, although we note that this problem may be of little concern for “big data” applications where SEs will likely be quite small.

Notwithstanding these limitations, the present research suggests that the regularized VAE is a feasible and promising approach to high-dimensional exploratory IFA for psychological and educational measurement, permitting computationally efficient estimation of large models that would be intractable using conventional

estimation techniques. Additionally, the VAE approach has many other compelling benefits that are worthy of further exploration. VAEs are fitted in small batches of observations, letting researchers refine their understanding of the underlying factor pattern as more data is collected. Factor scores produced by VAEs may be used in conjunction with other ANNs for predicting important outcomes. The rapidly developing DL literature includes a huge number of extensions that could enhance modeling and estimation in a wide variety of contexts. We view VAEs as part of a progression that started with the linear models of classical test theory, transitioned to the partially non-linear models of IRT, and is now advancing to utilize the fully non-linear models available in machine learning. We hope our work will aid this progression by helping to spur a fruitful dialogue between the fields of machine learning and psychometrics.

## 8 Acknowledgements

We are extremely grateful to Dr. David Thissen for his extensive suggestions, feedback, and support.

This material is based upon work supported by the National Science Foundation Graduate Research Fellowship under Grant No. DGE-1650116.

## References

- Asparouhov, T. & Muthén, B. (2009). *Exploratory structural equation modeling*. doi:10.1080/10705510903008204
- Bengio, Y. (2012). Practical recommendations for gradient-based training of deep architectures, 437–478. doi:10.1007/978-3-642-35289-8-26
- Biesanz, J. C. & West, S. G. (2004). Towards understanding assessments of the big five: Multitrait-multimethod analyses of convergent and discriminant validity across measurement occasion and type of observer. *Journal of Personality*, 72(4), 845–876. doi:10.1111/j.0022-3506.2004.00282.x
- Bjorner, J. B., Chang, C. H., Thissen, D., & Reeve, B. B. (2007). Developing tailored instruments: Item banking and computerized adaptive assessment. *Quality of Life Research*, 16(SUPPL. 1), 95–108. doi:10.1007/s11136-007-9168-6
- Blei, D. M., Kucukelbir, A., & McAuliffe, J. D. (2017). Variational inference: A review for statisticians. *Journal of the American Statistical Association*, 112(518), 859–877. doi:10.1080/01621459.2017.1285773
- Bock, R. D. & Aitkin, M. (1981). Marginal maximum likelihood estimation of item parameters: Application of an EM algorithm. *Psychometrika*, 46(4), 443–459. doi:10.1007/BF02293801
- Bolt, D. M. (2005). Limited- and full-information estimation of item response theory models. In A. Maydeau-Olivares & J. J. McArdle (Eds.), *Contemporary psychometrics* (Chap. 2, pp. 27–72). Mahwah, New Jersey: Lawrence Erlbaum Associates, Inc.

- Bottou, L. & Bousquet, O. (2011). The tradeoffs of large-scale learning. In *Optimization for machine learning* (Chap. 13). MIT Press.
- Bottou, L., Curtis, F. E., & Nocedal, J. (2018). Optimization methods for large-scale machine learning. *SIAM Review*, *60*(2), 223–311. doi:10.1137/16M1080173
- Bowman, S. R., Vilnis, L., Vinyals, O., Dai, A. M., Jozefowicz, R., & Bengio, S. (2016). Generating sentences from a continuous space. *Conference on Computational Natural Language Learning, Proceedings*, 10–21. doi:10.18653/v1/k16-1002
- Browne, M. W. (2001). An overview of analytic rotation in exploratory factor analysis. *Multivariate Behavioral Research*, *36*(1), 111–150. doi:10.1207/S15327906MBR3601\_05
- Cai, L. (2010a). High-dimensional exploratory item factor analysis by a Metropolis-Hastings Robbins-Monro algorithm. *Psychometrika*, *75*(1), 33–57. doi:10.1007/s11336-009-9136-x
- Cai, L. (2010b). Metropolis-Hastings Robbins-Monro algorithm for confirmatory item factor analysis. *Journal of Educational and Behavioral Statistics*, *35*(3), 307–335. doi:10.3102/1076998609353115
- Center for Behavioral Health Statistics and Quality. (2018a). *2017 National Survey on Drug Use and Health Final Analytic File Codebook*. Rockville, MD.
- Center for Behavioral Health Statistics and Quality. (2018b). *2017 National Survey on Drug Use and Health: Methodological Summary and Definitions*. Rockville, MD.
- Chen, C. M., Yoon, Y. H., Harford, T. C., & Grant, B. F. (2017). Dimensionality of DSM-5 posttraumatic stress disorder and its association with suicide attempts: results from the National Epidemiologic Survey on Alcohol and Related Conditions-III. *Social Psychiatry and Psychiatric Epidemiology*, *52*(6), 715–725. doi:10.1007/s00127-017-1374-0
- Choi, J., Oehlert, G., & Zou, H. (2010). A penalized maximum likelihood approach to sparse factor analysis. *Statistics and Its Interface*, *3*(4), 429–436. doi:10.4310/sii.2010.v3.n4.a1
- Christensen, R. H. B. (2019). Cumulative link models for ordinal regression with the R package ordinal. *Journal of Statistical Software*, (Christensen 2018), 1–40. Retrieved from www.jstatsoft.org/
- Curi, M., Converse, G. A., & Hajewski, J. (2019). Interpretable variational autoencoders for cognitive models. (July), 14–19.
- Desimone, J. A., Harms, P. D., & Desimone, A. J. (2015). Best practice recommendations for data screening. *Journal of Organizational Behavior*, *36*(2), 171–181. doi:10.1002/job.1962
- Fang, Y., Xu, J., & Yang, L. (2018). Online bootstrap confidence intervals for the stochastic gradient descent estimator. *Journal of Machine Learning Research*, *19*, 1–21.
- Gelfand, A. E. & Smith, A. F. (1990). Sampling-based approaches to calculating marginal densities. *Journal of the American Statistical Association*, *85*(410), 398–409. doi:10.1080/01621459.1990.10476213

- Glorot, X., Bordes, A., & Bengio, Y. (2011). Deep sparse rectifier neural networks. *Proceedings of Machine Learning Research*, 15, 315–323. doi:10.1.1.208.6449. arXiv: 1502.03167
- Goldberg, L. R. (1992). The development of markers for the Big-Five factor structure. *Psychological Assessment*, 4(1), 26–42.
- Goldberg, L. R., Johnson, J. A., Eber, H. W., Hogan, R., Ashton, M. C., Cloninger, C. R., & Gough, H. G. (2006). The international personality item pool and the future of public-domain personality measures. *Journal of Research in Personality*, 40(1), 84–96. doi:10.1016/j.jrp.2005.08.007
- Goodfellow, I., Bengio, Y., & Courville, A. (2016). *Deep learning*. Cambridge, MA: MIT Press. Retrieved from <http://www.deeplearningbook.org>
- Griewank, A. (2012). Who invented the reverse mode of differentiation? *Documenta Mathematica*, 1, 389–400.
- Hastings, W. K. (1970). Monte Carlo sampling methods using Markov chains and their applications. *Biometrika*, 57(1), 97–109.
- He, K., Zhang, X., Ren, S., & Sun, J. (2015). Delving deep into rectifiers: Surpassing human-level performance on ImageNet classification. *Proceedings of the IEEE International Conference on Computer Vision*, 1026–1034. doi:10.1109/ICCV.2015.123
- Heaton, J. (2008). *Introduction to Neural Networks for Java* (2nd ed.). Chesterfield, MO: Heaton Research, Inc.
- Hoffman, M. D., Blei, D. M., Wang, C., & Paisley, J. (2013). Stochastic variational inference. *Journal of Machine Learning Research*, 14, 1303–1347.
- Jain, P., Nagaraj, D., & Netrapalli, P. (2019). SGD without replacement: Sharper rates for general smooth convex functions, 1–14. Retrieved from <http://arxiv.org/abs/1903.01463>
- Jarrett, K., Kavukcuoglu, K., Ranzato, M., & LeCun, Y. (2009). What is the best multi-stage architecture for object recognition? *Proceedings of the IEEE International Conference on Computer Vision*.
- Kingma, D. P., Salimans, T., Jozefowicz, R., Chen, X., Sutskever, I., & Welling, M. (2016). Improved variational inference with inverse autoregressive flow. *Advances in Neural Information Processing Systems*, 4743–4751.
- Kingma, D. P. & Welling, M. (2013). Auto-encoding variational Bayes, 1–14. arXiv: 1312.6114. Retrieved from <http://arxiv.org/abs/1312.6114>
- Knafelz, G. J. & Grey, M. (2010). Factor analysis model evaluation through likelihood cross-validation. *Statistical Methods in Medical Research*, 16(2), 77–102.
- Lee, J. D., Simchowitz, M., Jordan, M. I., & Recht, B. (2016). Gradient descent converges to minimizers. *Journal of Machine Learning Research: Workshop and Conference Proceedings*, 49, 1–12. Retrieved from <http://arxiv.org/abs/1602.04915>
- Lord, F. M., Novick, M. R., & Birnbaum, A. (1968). *Statistical Theories of Mental Health Scores*. Oxford, England: Addison-Wesley.
- Lorenzo-Seva, U. & ten Berge, J. M. (2006). Tucker’s congruence coefficient as a meaningful index of factor similarity. *Methodology*, 2(2), 57–64. doi:10.1027/1614-2241.2.2.57

- Lu, Z., Pu, H., Wang, F., Hu, Z., & Wang, L. (2017). The expressive power of neural networks: A view from the width. *Conference on Neural Information Processing Systems*. Retrieved from <http://arxiv.org/abs/1709.02540>
- McNeish, D. M. (2015). Using lasso for predictor selection and to assuage overfitting: A method long overlooked in behavioral sciences. *Multivariate Behavioral Research*, *50*(5), 471–484. doi:10.1080/00273171.2015.1036965
- Meade, A. W. & Craig, S. B. (2012). Identifying careless responses in survey data. *Psychological Methods*, *17*(3), 437–455. doi:10.1037/a0028085
- Metropolis, N., Rosenbluth, A. W., Rosenbluth, M. N., Teller, A. H., & Teller, E. (1953). Equation of state calculations by fast computing machines. *The Journal of Chemical Physics*, *21*(6), 1087–1092. doi:10.1063/1.1699114
- Nair, V. & Hinton, G. E. (2010). Rectified linear units improve restricted Boltzmann machines. *International Conference on Machine Learning*, (3). doi:10.1.1.165.6419
- Nazabal, A., Olmos, P. M., Ghahramani, Z., & Valera, I. (2018). Handling incomplete heterogeneous data using VAEs, 1–19. Retrieved from <http://arxiv.org/abs/1807.03653>
- Niessen, A. S. M., Meijer, R. R., & Tendeiro, J. N. (2016). Detecting careless respondents in web-based questionnaires: Which method to use? *Journal of Research in Personality*, *63*, 1–11. doi:10.1016/j.jrp.2016.04.010
- Parikh, N. (2013). *Proximal algorithms*. doi:10.1561/2400000003
- Paszke, A., Gross, S., Chintala, S., Chanan, G., Yang, E., DeVito, Z., . . . Lerer, A. (2017). Automatic differentiation in PyTorch. *Workshop on Neural Information Processing Systems*. doi:10.1145/24680.24681
- Pinheiro, J. C. & Bates, D. M. (1996). Unconstrained parametrizations for variance-covariance matrices. *Statistics and Computing*, *6*(3), 289–296. doi:10.1007/BF00140873
- Prechelt, L. (2012). Early stopping - But when? In *Neural networks: tricks of the trade* (2nd, Chap. 2, pp. 53–67). Berlin, Heidelberg: Springer Verlag. doi:10.1007/978-3-642-35289-8-5
- Reddi, S. J., Kale, S., & Kumar, S. (2018). On the convergence of ADAM and beyond. *International Conference on Learning Representations*. Retrieved from <http://arxiv.org/abs/1904.09237>
- Reddi, S. J., Sra, S., Póczos, B., & Smola, A. J. (2016). Proximal stochastic methods for nonsmooth nonconvex finite-sum optimization. *Advances in Neural Information Processing Systems*, (2), 1153–1161.
- Reeve, B. B., Hays, R. D., Bjorner, J. B., Cook, K. F., Crane, P. K., Teresi, J. A., . . . Cella, D. (2007). Psychometric evaluation and calibration of health-related quality of life item banks: Plans for the Patient-Reported Outcomes Measurement Information System (PROMIS). *Medical Care*, *45*(5 SUPPL. 1), 22–31. doi:10.1097/01.mlr.0000250483.85507.04
- Reininghaus, U., Böhnke, J. R., Hosang, G., Farmer, A., Burns, T., McGuffin, P., & Bentall, R. P. (2016). Evaluation of the validity and utility of a transdiagnostic psychosis dimension encompassing schizophrenia and bipolar disorder. *British Journal of Psychiatry*, *209*(2), 107–113. doi:10.1192/bjp.bp.115.167882

- Reise, S. P. (2012). The rediscovery of bifactor measurement models. *Multivariate Behavioral Research*, *47*(5), 667–696. doi:10.1080/00273171.2012.715555
- Rezende, D. J., Mohamed, S., & Wierstra, D. (2014). Stochastic backpropagation and approximate inference in deep generative models. *Proceedings of the 31st International Conference on Machine Learning*, *32*(2), 1278–1286.
- Robbins, H. & Monro, S. (1951). A stochastic approximation method. *The Annals of Mathematical Statistics*, 400–407.
- Samejima, F. (1969). Estimation of latent ability using a response pattern of graded scores. *Psychometrika*, *35*(1), 139. doi:10.1007/BF02290599
- Scharf, F. & Nestler, S. (2019). Should regularization replace simple structure rotation in exploratory factor analysis? *Structural Equation Modeling*, *26*(4), 576–590. doi:10.1080/10705511.2018.1558060
- Shamir, O. (2016). Without-replacement sampling for stochastic gradient methods. *Advances in Neural Information Processing Systems*, 46–54.
- Shevlin, M., McElroy, E., Bentall, R. P., Reininghaus, U., & Murphy, J. (2017). The psychosis continuum: Testing a bifactor model of psychosis in a general population sample. *Schizophrenia Bulletin*, *43*(1), 133–141. doi:10.1093/schbul/sbw067
- Smith, L. N. (2018). *A disciplined approach to neural network hyper-parameters: Part 1 - learning rate, batch size, momentum, and weight decay*. US Naval Research Laboratory. arXiv: 1803.09820. Retrieved from <http://arxiv.org/abs/1803.09820>
- Sønderby, C. K., Raiko, T., Maaløe, L., Sønderby, S. K., & Winther, O. (2016). Ladder variational autoencoders. *Advances in Neural Information Processing Systems*, 3745–3753.
- Tibshirani, R. (1996). Regression shrinkage and selection via the lasso. *Journal of the Royal Statistical Society, Series B (Methodological)*, *58*(1), 267–288.
- Trendafilov, N. T. (2014). From simple structure to sparse components: A review. *Computational Statistics*, *29*(3-4), 431–454. doi:10.1007/s00180-013-0434-5
- Urban, C. J. & Gates, K. M. (2019). Deep learning : A primer for psychologists. doi:<https://doi.org/10.31234/osf.io/4q8na>
- van der Linden, D., te Nijenhuis, J., & Bakker, A. B. (2010). The General Factor of Personality: A meta-analysis of Big Five intercorrelations and a criterion-related validity study. *Journal of Research in Personality*, *44*(3), 315–327. doi:10.1016/j.jrp.2010.03.003
- Westling, T. & McCormick, T. H. (2019). Beyond prediction: A framework for inference with variational approximations in mixture models. *Journal of Computational and Graphical Statistics*, 1–39. doi:10.1080/10618600.2019.1609977. arXiv: 1510.08151
- Wirth, R. J. & Edwards, M. C. (2007). Item factor analysis: Current approaches and future directions. *Psychological Methods*, *12*(1), 58–79. doi:10.1037/1082-989X.12.1.58
- Yamamoto, M., Hirose, K., & Nagata, H. (2017). Erratum to: Graphical tool of sparse factor analysis. *Behaviormetrika*, *44*(1), 251–251. doi:10.1007/s41237-017-0017-9

Zhang, C., Butepage, J., Kjellstrom, H., & Mandt, S. (2019). Advances in variational inference. *IEEE Transactions on Pattern Analysis and Machine Intelligence*, 41(8), 2008–2026. doi:10.1109/TPAMI.2018.2889774